



# Synthesis of a polymer-capped palladium nanoparticles and its application as a reusable catalyst in oxidative coupling reaction of $\alpha$ -hydroxyketones and 1,2-diamines for preparation of pyrazines and quinoxalines

Mohammad Ali Karimi Zarchi<sup>1</sup> · Seyed Shahab Addin Darbandizadeh Mohammad Abadi<sup>1</sup>

Received: 19 November 2017 / Accepted: 2 January 2018 / Published online: 23 January 2018  
© Iranian Chemical Society 2018

## Abstract

A novel method for the synthesis of pyrazines and quinoxalines has been developed using  $\alpha$ -hydroxyketones and 1,2-diamines in the presence of cross-linked poly(4-vinylpyridine)-stabilized Pd(0) nanoparticles, [P4-VP]-PdNPs. The catalyst was easily prepared and characterized using various techniques such as FT-IR and UV–Vis spectroscopy, AAS, TEM, FESEM, EDX analysis and XRD. The results confirm a good dispersion of palladium nanoparticles on the polymer support. The catalyst displayed good catalytic activity when applied to the synthesis of quinoxalines via condensation of  $\alpha$ -hydroxyketones with 1,2-diamines. A few pyrazine derivatives and various quinoxalines are prepared via coupling reaction of  $\alpha$ -hydroxyketones and 1,2-diamines in high–excellent yields (81–99%) with short reaction times. The quinoxalines products were characterized by FT-IR, <sup>1</sup>H and <sup>13</sup>C NMR spectroscopy, and the physical properties were compared to the literature values of known compounds. The advantages of the present method over conventional classical methods are rapid and very simple work-up, and the catalyst is reusable many times without a significant loss in its activity.

**Keywords** Pyrazine · Quinoxaline · Characterization · Benzoin · Palladium nanoparticle

## Introduction

Quinoxaline derivatives are an important class of heterocyclic compounds, in which two nitrogen atoms are replaced by carbon atoms at 1 and 4 positions of the naphthalene ring. The study of quinoxaline and its derivatives has become a subject of interest in recent years due to their wide variety of biological activities as well as therapeutic applications [1, 2]. For example, they can be used against bacteria, fungi, virus, leishmania, tuberculosis, malaria, cancer, depression, neurological activities, among others [3–6].

Also, quinoxaline moieties are present in the structure of various antibiotics such as echinomycin, levomycin and actinoleutin, which are known to inhibit the growth of gram-positive bacteria, and they are active against various transplantable tumors [7, 8]. They also serve as useful rigid subunits

in macrocyclic receptors in molecular recognition [9]. In addition, quinoxaline derivatives have also found applications in dyes, organic semiconductors, chemically controllable switches and efficient electron luminescent materials [10–13]. Considering their chemical and biological significance, numerous synthetic strategies have been developed for the preparation of quinoxaline derivatives and the vast scope of synthesized quinoxaline and derivatives potential is well referenced and published in a wide range of scientific journals. Scientific data concerning the potential relevance of quinoxaline and derivatives in the literature were analyzed. The most common method for the synthesis of quinoxaline derivatives is the coupling reaction of 1,2-dicarbonyles and *o*-phenylenediamines in the presence of an acidic catalysts [14–18]. Also, numerous methods are available for the synthesis of quinoxaline derivatives which involve condensation of 1,2-diamines with  $\alpha$ -diketones [19–21], oxidative coupling of epoxides with ene-1,2-diamines [22, 23] and cyclization–oxidation of phenacyl bromides [24, 25]. Also,  $\alpha$ -hydroxyketones react with *o*-phenylenediamines in the presence of transition metals such as Ru and Pd to give

✉ Mohammad Ali Karimi Zarchi  
makarimi@yazd.ac.ir

<sup>1</sup> Department of Chemistry, College of Science, Yazd University, P. O. Box 89195-741, 8915813149 Yazd, Iran

quinoxalines [26]. However, many of these processes suffer from one or more limitations such as low product yields, tedious work-up procedures, drastic reaction conditions, the use of toxic metal salts as catalysts, and relatively expensive reagents.

Palladium nanoparticles used in C–C coupling reactions are usually formed by metal salt reduction and are generally stabilized by polymeric molecules, tetraalkylammonium salts and ionic liquids. Very recently, palladium dispersions containing small metal particles (20–80 Å) have been of increasing scientific interest as a colloidal catalyst for organic C–C bond formation reactions (Heck reactions) [27, 28]. In recent years, the polymeric catalysts, reagents and scavengers have been widely applied in organic transformations [29–69]. Also there are many reports on polymer-supported palladium in the literature [51–69]. Poly(vinylpyrrolidone) (PVP) has been shown to be an effective matrix in stabilizing palladium nanoparticles as catalyst for cross-coupling reactions such as coupling of aryl iodides with arylboronic acid [52, 53], Suzuki reactions [54–57], Sonogashira reaction [58], Heck and carbonylation reactions [55, 59, 60], hydrogenation of 2-ethyl-9,10-anthraquinone [61], electroless copper deposition [62], nitrate and nitrite reduction [63] and H–D exchange between N-heterocyclic compounds and D<sub>2</sub>O [64]. Palladium nanoparticles supported on poly(*N*-vinylpyrrolidone)-grafted silica as new recyclable catalyst for Heck cross-coupling reactions also was reported by Tamami et al. [66]. Also in 2011, Iyer and co-workers reported synthesis of palladium nanoparticles assembled in a polymeric nanosphere as catalyst for the Mizoroki–Heck cross-coupling reaction [67]. In 2014, Kaur and Shah reported the microwave-assisted fluoride-free Hiyama cross-coupling reaction catalyzed by Pd(0)–PVP nanoparticles [68]. In 2014, Lefferts and co-workers reported PVP-stabilized Pd nanoparticles as catalyst for nitrite hydrogenation in aqueous phase [69].

The recent developments in polymer-supported reactions have led to the propagation of combinatorial chemistry as a method for the rapid and efficient preparation of novel functionalized molecules [29]. A fast growing branch of this area is polymer-supported catalysts, reagents and scavengers [30]. Although there are numerous applications of polymeric catalysts in literature but, to the best of our knowledge, there is no report for the synthesis of quinoxaline derivatives by using polymer-supported palladium particles via oxidative

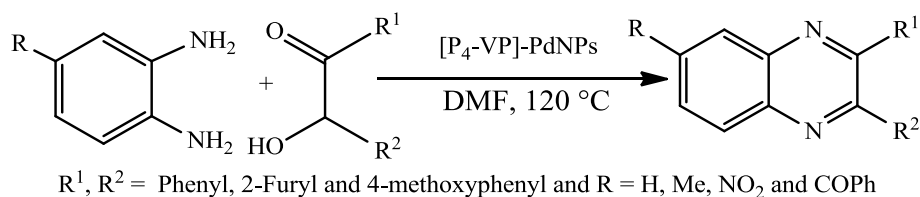
coupling reaction of  $\alpha$ -hydroxyketones and 1,2-diamines. Hence, in continuation of our studies on organic transformations using polymer-supported catalysts, reagents and scavengers based on commercially available cross-linked poly(4-vinylpyridine) [32–50], in the present study, we wish to report preparation, characterization and catalytic application of cross-linked poly(4-vinylpyridine)-supported palladium nanoparticles abbreviated as [P<sub>4</sub>-VP]-PdNPs as a new recyclable catalyst in organic transformations. Also, herein we wish to report a one-pot oxidation–condensation method for the synthesis of pyrazines and quinoxalines from readily available benzoin and 1,2-diamines by heating in DMF (Scheme 1).

## Experimental

### Material

Chemicals were either prepared in our laboratory or were purchased from Fluka (Buchs, Switzerland), Aldrich (Milwaukee, WI) and Merck chemical companies and were used without further purification. Poly(4-vinylpyridine) cross-linked with 2% divinyl benzene (DVB), [P<sub>4</sub>-VP] 2% DVB, was purchased from Fluka company (Buchs, Switzerland), and [P<sub>4</sub>-VP]-PdNPs was prepared in our laboratory as described below and characterized by FT-IR, ultraviolet–visible spectrophotometry (UV–Vis), atomic absorption spectrometer (AAS) transmission electron microscopy images (TEM), field emission scanning electron microscopy (FESEM) images, energy-dispersive X-ray analysis spectroscopy (EDX) and X-ray powder diffraction (XRD). The reactions were monitored by thin layer chromatography (TLC) using silica gel Poly Gram SIL G/UV 254 plates. All products were characterized by comparison of their FT-IR, proton and carbon thirteen nuclear magnetic resonance (<sup>1</sup>H- and <sup>13</sup>C NMR) spectra and physical data with pure compounds. All yields refer to the isolated products. The FT-IR spectra were obtained with a Bruker Equinox (model 55, Germany), and the NMR spectra were recorded on a Bruker AC 400 Avance DPX spectrophotometer (Germany) at 400 MHz for <sup>1</sup>H and at 100 MHz for <sup>13</sup>C NMR in CDCl<sub>3</sub> solutions and on a Bruker (DRX-500 AVANCE) 500 MHz spectrometer at 500 MHz for <sup>1</sup>H and at 125 MHz for <sup>13</sup>C NMR in CDCl<sub>3</sub> (using tetramethylsilane as internal reference). Capacity

**Scheme 1** Synthesis of pyrazines and quinoxalines



measurements were carried out with an Analytik Jena nova 300 (model 330, Germany) atomic absorption spectrometer utilizing an air-acetylene flame atomizer. The UV–Vis absorption spectra were recorded on an Avantes photodiode array spectrophotometer model AvaSpec-2048 equipped with a source model of AvaLight-DH-S-BAL. TEM images were recorded using ZEISS 10A conventional TEM model Carl Zeiss-EM10C-100 kV (Germany). FESEM images were recorded using FESEM MIRA 3-XMU with a high-energy beam of electrons from Razi Metallurgical Research Center. EDX analysis was performed using ZEISS (model SIGMA VP-500, Germany) with Oxford Instrument detector (England). XRD patterns were recorded on a PANalytical (model X'Pert PRO) X-ray diffractometer. The uncorrected melting points of compounds were taken by a Buchi melting point B-540 B.V. CHI apparatus.

### Preparation of [P<sub>4</sub>-VP]-PdNPs

The [P<sub>4</sub>-VP]-PdNPs were prepared by the following procedure: In the first step, aqueous solution of H<sub>2</sub>PdCl<sub>4</sub> was prepared by mixing 106.4 mg of PdCl<sub>2</sub> (0.6 mmol), 6.0 mL of 0.2 M HCl and 294 mL of distilled water. In the second step, a mixture of 15 mL solution of H<sub>2</sub>PdCl<sub>4</sub> (prepared in the first step), 21 mL of methanol and 0.2668 g of [P<sub>4</sub>-VP] 2% DVB was refluxed in a 100-mL flask for 1 h. In the final step, 15 ml of 0.015 M solution of sodium borohydride in methanol was added into the above mixture dropwise immediately. The abrupt color change from pale green to dark brown indicates that Pd<sup>2+</sup> reduced to Pd(0) nanoclusters stabilized by [P<sub>4</sub>-VP] 2% DVB, and consequently, the [P<sub>4</sub>-VP]-PdNPs were formed. Methanol was removed from the solution by evaporation in a rotary evaporator (Heidolph Laborata-4000), and [P<sub>4</sub>-VP]-PdNPs were washed with excess acetone to remove the excess residuals.

### General procedure for synthesis of pyrazine or quinoxaline derivatives

A mixture of benzoin (1 mmol), *o*-phenylenediamine (1.1 mmol) and [P<sub>4</sub>-VP]-PdNPs (120 mg) was refluxed in DMF (3 mL). After completion of reaction (monitored by TLC, eluent: *n*-hexane/EtOAc = 9/1), the catalyst was separated and washed with EtOH (2 × 2 mL). After addition of water the product was precipitated with high purity. The pure quinoxalines were obtained in 81–99% isolated yields.

### Synthesis of 2,3-diphenylquinoxaline as a typical procedure (3a)

A mixture of benzoin (1 mmol), *o*-phenylenediamine (1.1 mmol) and [P<sub>4</sub>-VP]-PdNPs (120 mg) was refluxed in DMF (3 mL). After the completion of reaction (monitored

by TLC, eluent: *n*-hexane/EtOAc = 9/1), the catalyst was separated and washed with EtOH (2 × 2 mL). After the addition of water, the product was precipitated with high purity. The pure quinoxalines were obtained in 95% isolated yield.

The characteristic spectral data of some quinoxalines products are given below, and the FT-IR, <sup>1</sup>H and <sup>13</sup>C NMR spectra of 6-benzoyl-2,3-difuran-2-yl-quinoxaline (3i), for example, are given in Fig. 1a–c.

**2,3-Diphenylquinoxaline (3a)** White solid, m.p. = 127–128 °C (lit; 127–129 [70], 126–127 °C [71] and 128–129 °C [72]); FT-IR (neat),  $\nu_{\max}$  (cm<sup>-1</sup>) = 3053, 3026, 1620, 1556, 1533, 1483, 1445, 1344, 1308, 1202, 1138, 1061, 1022, 980, 833, 817, 775, 752, 704, 696, 596, 546; <sup>1</sup>H NMR (400 MHz, CDCl<sub>3</sub>),  $\delta$  (ppm) = 8.19–8.23 (m, 2H), 7.78–7.83 (m, 2H), 7.52–7.57 (m, 4H), 7.34–7.41 (m, 6H); <sup>13</sup>C NMR (100 MHz, CDCl<sub>3</sub>),  $\delta$  (ppm) = 153.49, 141.25, 139.09, 129.98, 129.85, 129.22, 128.82, 128.29.

**6-Methyl-2,3-diphenylquinoxaline (3b)** White solid, m.p. = 115–117 °C (lit. 116–117 °C [71] and 117–118 °C [72]); FT-IR (neat),  $\nu_{\max}$  (cm<sup>-1</sup>) = 3055, 2924, 2853, 1556, 1541, 1440, 1346, 1219, 1059, 978, 770, 760, 731, 700, 600, 542; <sup>1</sup>H NMR (400 MHz, CDCl<sub>3</sub>),  $\delta$  (ppm) = 2.6 (s, 3H), 7.32 (m, 6H), 7.52 (m, 4H), 7.57 (d, *J* = 8.75 Hz, 1H), 7.96 (s, 1H), 8.05 (d, *J* = 8.5 Hz, 1H); <sup>13</sup>C NMR (100 MHz, CDCl<sub>3</sub>),  $\delta$  = 21.9, 127.1, 128.2, 128.6, 128.7, 129.8, 132.3, 139.2, 139.7, 140.4, 141.3, 152.5, 153.3.

**6-Nitro-2,3-diphenylquinoxaline (3c)** White solid, m.p. = 193–194 °C (lit. 192–193 °C [71], 193–194 °C [72] and 183 °C [73]); FT-IR (neat),  $\nu_{\max}$  (cm<sup>-1</sup>) = 3090, 3055, 2953, 2924, 2853, 1616, 1570, 1520, 1466, 1435, 1398, 1336, 1310, 1285, 1244, 1207, 1186, 1163, 1128, 1072, 1055, 1026, 980, 907, 812, 798, 745, 700, 635, 598, 540; <sup>1</sup>H NMR (400 MHz, CDCl<sub>3</sub>),  $\delta$  (ppm) = 7.43 (m, 6H), 7.60 (t, *J* = 6.5 Hz, 4H), 8.33 (d, *J* = 9.1 Hz, 1H), 8.56 (dd, *J* = 9.1, 2.2 Hz, 1H), 9.19 (d, *J* = 2.3 Hz, 1H); <sup>13</sup>C NMR (100 MHz, CDCl<sub>3</sub>),  $\delta$  (ppm) = 123.73, 126.06, 128.89, 130.07, 130.20, 130.26, 130.33, 131.192, 138.47, 138.54, 140.42, 144.02, 148.32, 156.13, 156.75.

**6-Benzoyl-2,3-diphenylquinoxaline (3d)** White solid, m.p. = 149–151 °C (lit. 139–140 °C [73]); FT-IR (neat),  $\nu_{\max}$  (cm<sup>-1</sup>) = 3055, 1661, 1597, 1445, 1346, 1321, 1310, 1288, 1265, 1246, 1225, 1198, 1180, 1124, 1074, 1057, 1022, 980, 907, 891, 793, 770, 733, 716, 696, 675, 600, 452; <sup>1</sup>H-NMR (400 MHz, CDCl<sub>3</sub>),  $\delta$  (ppm) = 7.30 (m, 6H), 7.47 (m, 7H), 7.83 (m, 2H), 7.83 (dd, *J* = 8 and 1.4 Hz, 2H), 8.21 (m, 2H), 8.47 (s, 1H); <sup>13</sup>C-NMR (100 MHz, CDCl<sub>3</sub>),  $\delta$  (ppm) = 128.41, 128.55, 129.21, 129.36, 129.70, 129.79, 129.92, 130.16, 132.46, 132.85, 137.18, 138.36, 138.52, 138.58, 140.19, 142.92, 154.63, 155.14, 195.82.

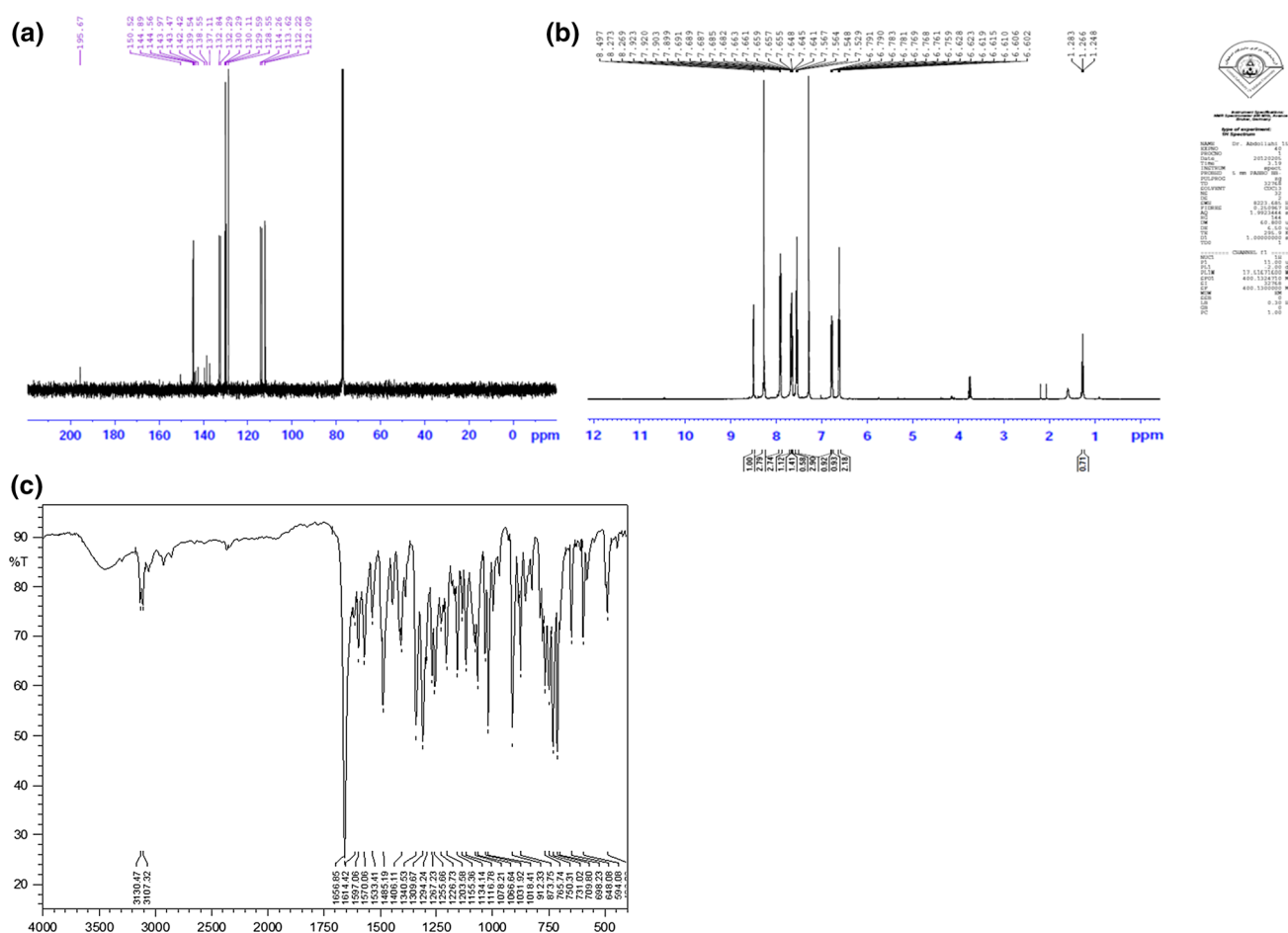


**Fig. 1** FT-IR, <sup>1</sup>H and <sup>13</sup>C NMR spectra of 6-benzoyl-2,3-difuran-2-yl-quinoxaline (**a–c**)

**2,3-Dihydro-5,6-diphenylpyrazine (3e)** White solid, m.p. = 160–162 °C (lit. 158 °C [17] and 160–163 [70]); FT-IR (neat),  $\nu_{\max}$  (cm<sup>-1</sup>) = 3090, 3055, 2953, 2924, 1616, 1570, 1520, 1466, 1435, 1398, 1338, 1309, 1284, 1244, 1207, 1186, 1163, 1128, 1072, 1055, 1026, 980, 906, 812, 768, 745, 700, 635, 598, 540; <sup>1</sup>H NMR (400 MHz, CDCl<sub>3</sub>),  $\delta$  (ppm) = 3.73 (s, 4H), 7.28 (t,  $J$  = 7.5 Hz, 4H), 7.34 (t,  $J$  = 7 Hz, 2H), 7.43 (d,  $J$  = 7.5 Hz, 4H); <sup>13</sup>C NMR (100 MHz, CDCl<sub>3</sub>),  $\delta$  (ppm) = 46.25, 128.33, 128.54, 130.05, 138.21, 160.73.

**2,3-Difuran-2-yl-quinoxaline (3f)** Pale brown solid, m.p. = 132–134 °C (lit. 132–134 °C [70]); FT-IR (neat),  $\nu_{\max}$  (cm<sup>-1</sup>) = 3107, 1570, 1537, 1479, 1400, 1337, 1327, 1163, 1128, 1076, 1059, 1034, 1009, 993, 912, 762, 752, 596, 494; <sup>1</sup>H-NMR (400 MHz, CDCl<sub>3</sub>),  $\delta$  (ppm) = 6.59 (m, 2H); 6.7 (d,  $J$  = 3.31 Hz, 2H), 7.6 (d,  $J$  = 1.02 Hz, 2H), 7.78 (m, 2H); 8.17 (m, 2H); <sup>13</sup>C NMR (125 MHz, CDCl<sub>3</sub>),  $\delta$  (ppm) = 112.35, 113.43, 129.56, 130.83, 141.074, 143.09, 144.66, 151.25.

**6-Methyl-2,3-difuran-2-yl-quinoxaline (3g)** Pale brown solid, m.p. = 119–120 °C (lit. 119–120 °C [70]); FT-IR (neat),  $\nu_{\max}$  (cm<sup>-1</sup>) = 3111, 2922, 1618, 1570, 1533, 1491, 1458, 1404, 1337, 1217, 1167, 1150, 1134, 1076, 1062, 1018, 991, 912, 887, 829, 820, 800, 758, 748, 598, 582, 490; <sup>1</sup>H-NMR (400 MHz, CDCl<sub>3</sub>),  $\delta$  (ppm) = 2.52 (s, 3H), 6.48–6.49 (m, 2H), 6.5 (m, 2H), 7.51 (dd,  $J$  = 8.6, 1.8 Hz, 2H), 7.54 (m, 1H), 7.84 (s, 1H), 7.95 (d,  $J$  = 8.4 Hz, 1H); <sup>13</sup>C-NMR (100 MHz, CDCl<sub>3</sub>),  $\delta$  (ppm) = 21.95, 111.87, 111.89, 112.58, 112.83, 127.99, 128.64, 132.80, 139.12, 140.74, 141.14, 141.87, 142.62, 144.01, 144.14, 150.92.

**6-Nitro-2,3-difuran-2-yl-quinoxaline (3h)** Orange solid, m.p. = 167–169 °C (lit. 171–173 °C [70] and 164–166 °C [73]); FT-IR (neat),  $\nu_{\max}$  (cm<sup>-1</sup>) = 3119, 2924, 1616, 1566, 1519, 1485, 1402, 1387, 1346, 1296, 1254, 1215, 1157, 1080, 1063, 1022, 995, 951, 889, 841, 826, 754, 733, 592, 484; <sup>1</sup>H-NMR (400 MHz, CDCl<sub>3</sub>),  $\delta$  (ppm) = 6.65 (m, 2H), 6.85 (dd,  $J$  = 3.4, 0.6 Hz, 1H), 6.91 (dd,  $J$  = 3.4, 0.6 Hz, 1H), 7.70 (m, 2H), 8.25 (d,  $J$  = 9.2 Hz, 2H), 8.51 (dd,  $J$  = 9.2,

3.2 Hz, 2H), 9.04 (d,  $J = 3.2$  Hz, 1H);  $^{13}\text{C}$  NMR (100 MHz,  $\text{CDCl}_3$ ),  $\delta$  (ppm) = 112.31, 112.44, 114.51, 115.37, 123.66, 125.37, 130.47, 139.26, 143.02, 144.23, 144.73, 145.01, 145.49, 147.95, 149.40, 150.17.

**6-Benzoyl-2,3-difuran-2-yl-quinoxaline (3i)** Pale brown solid, m.p. = 119 °C (lit. 118–120 °C [70]); FT-IR (neat),  $\nu_{\text{max}}$  ( $\text{cm}^{-1}$ ): 3130, 3107, 1657, 1614, 1597, 1570, 1533, 1485, 1406, 1341, 1310, 1294, 1267, 1256, 1227, 1204, 1155, 1134, 1117, 1087, 1067, 1032, 1018, 912, 874, 766, 750, 731, 710, 698, 648, 594;  $^1\text{H}$ -NMR (400 MHz,  $\text{CDCl}_3$ ),  $\delta$  (ppm) = 6.60–6.63 (m, 2H), 6.76–6.79 (m, 2H), 7.53–7.57 (m, 3H), 7.64–7.69 (m, 2H), 7.90–7.92 (m, 2H), 8.27 (d,  $J = 1.6$ , 2H), 8.5 (t,  $J = 1.2$ , 1H);  $^{13}\text{C}$  NMR (100 MHz,  $\text{CDCl}_3$ ),  $\delta$  (ppm) = 112.09, 112.22, 113.62, 114.26, 128.55, 129.59, 130.11, 132.29, 132.84, 137.11, 138.55, 139.54, 142.42, 143.47, 143.97, 144.56, 144.89, 150.52, 195.67.

**2,3-Bis(4-methoxyphenyl)quinoxaline (3j)** White solid, m.p. = 149–151 °C (lit. 151–152 °C [70], 148–150 °C [73] and 151–152.5 °C [72, 74]); FT-IR (neat),  $\nu_{\text{max}}$  ( $\text{cm}^{-1}$ ) = 3063, 3006, 2967, 2887, 2837, 1665, 1601, 1574, 1536, 1512, 1477, 1458, 1440, 1423, 1392, 1346, 1296, 1284, 1244, 1224, 1170, 1161, 1138, 1109, 1086, 1068, 1028, 977, 879, 829, 804, 786, 733, 670, 610, 588, 633;  $^1\text{H}$  NMR (500 MHz,  $\text{CDCl}_3$ ),  $\delta$  (ppm) = 3.8 (s, 6H), 6.91 (d,  $J = 6.73$  Hz, 4H), 7.53 (d,  $J = 6.63$  Hz, 4H), 7.76 (dd, 2H), 8.16 (dd, 2H);  $^{13}\text{C}$  NMR (125 MHz,  $\text{CDCl}_3$ ),  $\delta$  (ppm) = 55.74, 114.21, 129.44, 129.95, 131.68, 132.17, 141.51, 153.46, 160.60.

**6-Methyl-2,3-bis(4-methoxyphenyl)quinoxaline (3k)** White solid, m.p. = 128–130 °C (lit. 123–126 °C [70] and 125–127 °C [72, 74]); FT-IR (neat),  $\nu_{\text{max}}$  ( $\text{cm}^{-1}$ ) = 2953, 2926, 2837, 1655, 1607, 1573, 1512, 1187, 1458, 1344, 1288, 1248, 1178, 1163, 1028, 833;  $^1\text{H}$  NMR (400 MHz,  $\text{CDCl}_3$ ),  $\delta$  (ppm) = 2.52 (s, 3H), 3.75 (s, 6H), 6.79 (d,  $J = 7.2$ , 4H), 7.40 (d,  $J = 7.2$ , 4H), 7.47 (d,  $J = 7.6$  Hz, 1H), 7.84 (s, 1H), 7.93 (d,  $J = 7.6$  Hz, 1H);  $^{13}\text{C}$  NMR (100 MHz,  $\text{CDCl}_3$ ),  $\delta$  (ppm) = 21.89, 55.31, 113.74, 127.88, 128.53, 131.20, 131.24, 132.87, 139.54, 140.00, 141.14, 152.17, 152.90, 160.01.

**6-Nitro-2,3-bis(4-methoxyphenyl)quinoxaline (3l)** Orange solid, m.p. = 192–193 °C (lit. 192–194 °C [72] and 192–194 °C [74]); FT-IR (neat),  $\nu_{\text{max}}$  ( $\text{cm}^{-1}$ ) = 3005, 2926, 2853, 1607, 1574, 1516, 1466, 1435, 1342, 1305, 1294, 1251, 1177, 1020, 978, 847, 826, 679, 538.

**6-Benzoyl-2,3-bis(4-methoxyphenyl)quinoxaline (3m)** White solid, m.p. = 147–148 °C; FT-IR (neat),  $\nu_{\text{max}}$  ( $\text{cm}^{-1}$ ) = 2955, 2924, 2853, 1653, 1605, 1574, 1512, 1458, 1348, 1334,

1306, 1296, 1260, 1248, 1227, 1173, 1161, 1026, 835, 725, 712.

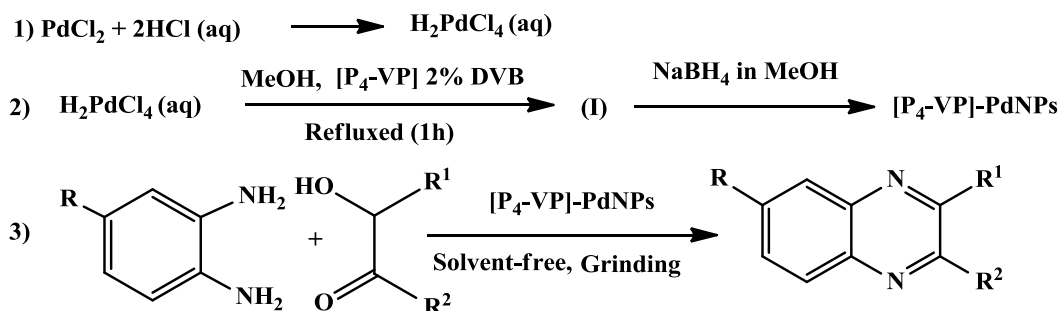
**5,6-Bis-(4-methoxyphenyl)-2,3-dihydro-pyrazin (3n)** Very pale brown solid, m.p. = 157–160 °C; FT-IR (neat),  $\nu_{\text{max}}$  ( $\text{cm}^{-1}$ ) = 3055, 1556, 1541, 1479, 1346, 1219, 1059, 978, 770, 760, 731, 700, 600, 542.

## Results and discussion

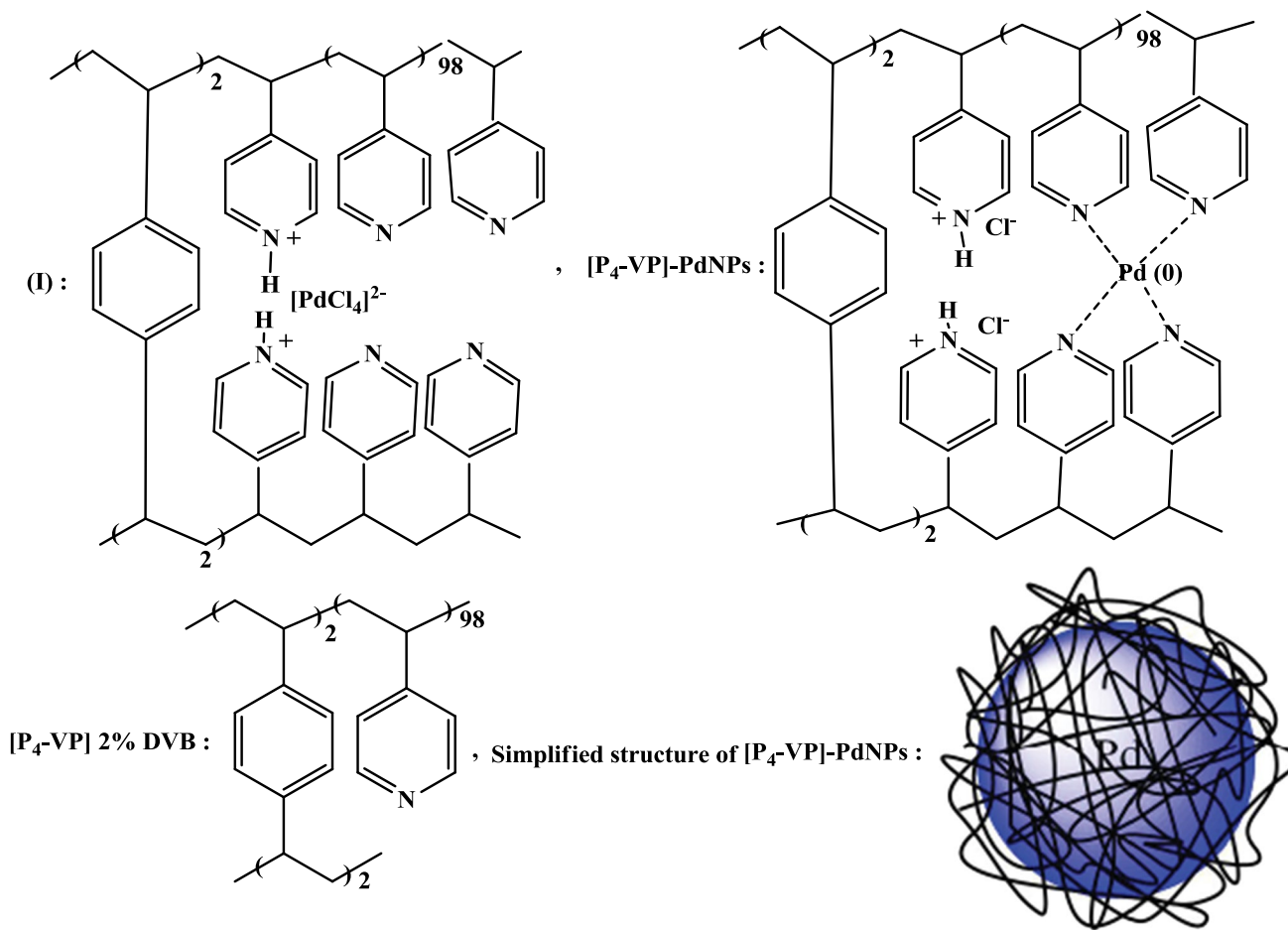
The palladium nanoparticles immobilized on cross-linked poly(4-vinylpyridine) was easily prepared in the two-step procedure. In the first step, aqueous solution of  $\text{H}_2\text{PdCl}_4$  was prepared by mixing  $\text{PdCl}_2$ ,  $\text{HCl}$  and distilled water (step 1, Scheme 2). Then, methanol and  $[\text{P}_4\text{-VP}]$  2% DVB were added to the above mixture and refluxed for 1 h. The UV–Vis electronic absorption spectrum of this solution shows that no reduction of  $\text{Pd}^{2+}$  species to  $\text{Pd}(0)$  occurs during the reflux (Fig. 2).

We also performed experiments to understand the effect of reflux in methanol on reduction of  $\text{Pd}^{2+}$  precursor varying the reflux time up to 3 h, but there was no reduction observed. It is clearly seen that reflux in methanol alone is not enough to reduce  $\text{Pd}^{2+}$  precursor to zero valent palladium. Therefore, sodium borohydride solution in methanol was added dropwise to the mixture to reduction of  $\text{Pd}^{2+}$  precursors to  $\text{Pd}(0)$  occurs. An abrupt color change was observed from pale yellow to dark brown immediately upon the addition of sodium borohydride, indicating decreasing cluster size and the formation of  $\text{Pd}(0)$  nanoclusters on the surface or in the pores of the polymer. But, when reflux in ethanol was used instead of methanol, we observed that reduction of  $\text{Pd}^{2+}$  species to  $\text{Pd}(0)$  occurs during the reflux and stabilized by polymer to produce the  $[\text{P}_4\text{-VP}]\text{-PdNPs}$  catalyst and we also observed (as expected) the  $\text{C}=\text{O}$  stretching frequency of acetaldehyde at  $1655\text{ cm}^{-1}$  in the FT-IR spectrum of the filtrates after the catalyst was separated by filtration. Our initial investigation on the evaluation of the catalytic activity of  $[\text{P}_4\text{-VP}]\text{-PdNPs}$  started with the coupling reaction between  $\alpha$ -hydroxyketones and 1,2-diamines for synthesis of quinoxalines, and we found that  $[\text{P}_4\text{-VP}]\text{-PdNPs}$  are a suitable and reusable catalyst for synthesis of quinoxalines (step 3, Scheme 2) and also we found that the  $[\text{P}_4\text{-VP}]\text{-PdNPs}$  are stable for months at room temperature in air and can be recovered and reused several cycles.

The catalyst was characterized using several techniques. The morphology and structure of the samples were examined by UV–Vis absorption spectra (Fig. 2), FT-IR spectroscopy (Fig. 3), TEM images (Fig. 4a, b), FESEM (Fig. 5a–c), EXD pattern (Fig. 5d) and XRD spectroscopy (Fig. 6) and AAS experimental techniques.



$\text{R}^1, \text{R}^2 = \text{Phenyl, 2-Furyl and 4-methoxyphenyl}$  and  $\text{R} = \text{H, Me, NO}_2 \text{ and COPh}$



**Scheme 2** Synthesis of  $[\text{P}_4\text{-VP}]\text{-PdNPs}$

Figure 2 shows the UV–Vis absorption spectra of (a)  $\text{H}_2\text{PdCl}_4$ , (b)  $[\text{P}_4\text{-VP}] \text{ 2\% DVB}$  after refluxed in methanol (1 h) in the presence of  $\text{H}_2\text{PdCl}_4$  before the addition of sodium borohydride (I, in Scheme 2) and (c) polymer after addition of sodium borohydride,  $[\text{P}_4\text{-VP}]\text{-PdNPs}$  (Scheme 2). As Fig. 2 reveals, two absorption bands observed at 250 and 325 nm attributed to the  $[\text{PdCl}_4]^{2-}$  anions (a and b) that disappeared when sodium borohydride was added to the mixture (c). This disappearance indicates that the reduction of  $\text{Pd}^{2+}$  precursor to  $\text{Pd}(0)$  occurs and stabilized by

$[\text{P}_4\text{-VP}] \text{ 2\% DVB}$ , and consequently, the  $[\text{P}_4\text{-VP}]\text{-PdNPs}$  catalyst forms. The free pyridine pendant group of  $[\text{P}_4\text{-VP}] \text{ 2\% DVB}$  can also be protonated by adsorbing the liberate  $\text{HCl}$  as a toxic waste. The structures of  $[\text{P}_4\text{-VP}] \text{ 2\% DVB}$  and  $[\text{P}_4\text{-VP}]\text{-PdNPs}$  and the simplified structure of  $[\text{P}_4\text{-VP}]\text{-PdNPs}$  are shown in Scheme 2.

Vibrational spectroscopy is a suitable tool for characterization of polymer-transition metal ions systems. It is known that the  $\text{C}=\text{N}$  and  $\text{C}=\text{C}$  stretching frequencies in vinylpyridine polymers shift to higher frequencies upon

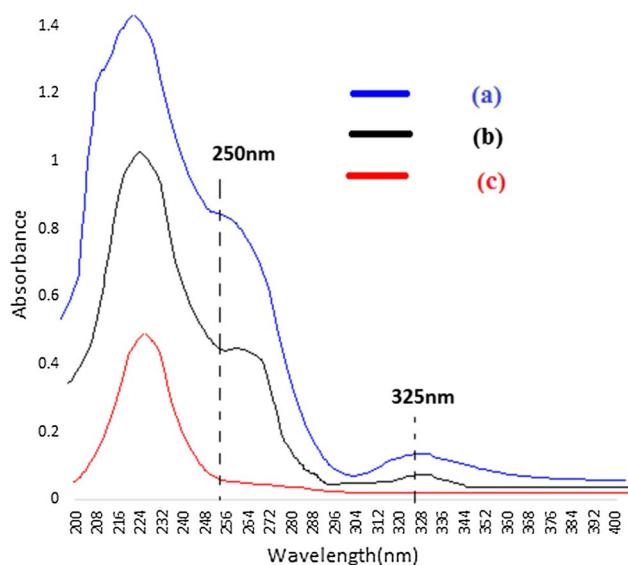


**Fig. 2** UV-Vis absorption spectra of **a**  $\text{H}_2\text{PdCl}_4$ , **b**  $[\text{P}_4\text{-VP}]$  2% DVB after refluxed (1 h) in  $\text{H}_2\text{PdCl}_4$  solution before the addition of sodium borohydride (I, in Scheme 2) and **c**  $[\text{P}_4\text{-VP}]$ -PdNPs

complexation with metal ions such as  $\text{Cu}^{2+}$  [37, 75] and  $\text{Pd}^{2+}$  ions [76]. Hasik et al. have studied the palladium–nitrogen-containing polymers interactions, and they have been found that, in the  $\text{PdCl}_2$  solutions of high HCl concentration containing  $[\text{PdCl}_4]^{2-}$  and  $[\text{PdCl}_3(\text{H}_2\text{O})]^-$  as the major species acid–base type reaction (protonation) as well as the coordination of  $\text{Pd}^{2+}$  ions by the nitrogen atoms of the polyvinylpyrrolidone take place. In the present study also, the nitrogen atoms of the pyridine rings in the structure of  $[\text{P}_4\text{-VP}]$  2% DVB constitute potential sites for polymer–palladium complexes interactions and also can be protonated by adsorbing the liberates HCl as a toxic waste to give the

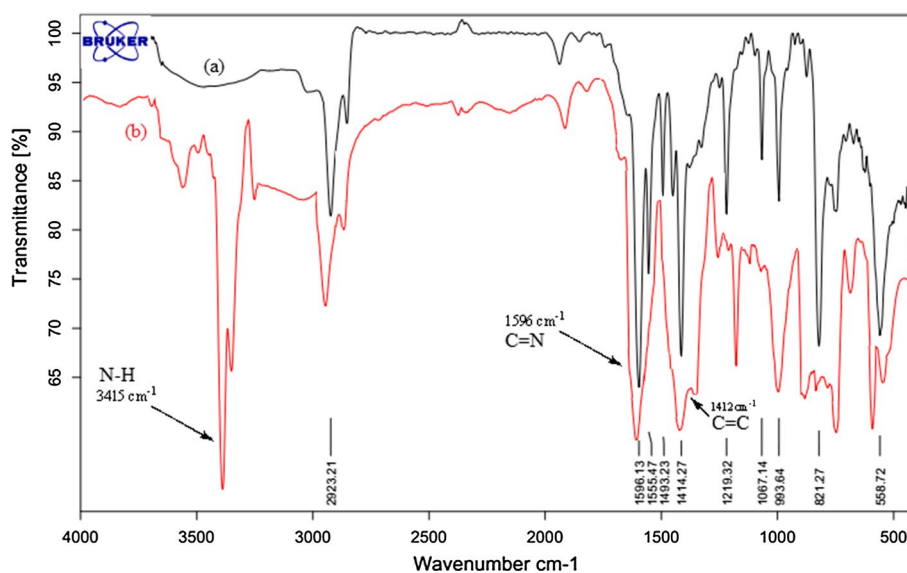
corresponding salt (I) and  $[\text{P}_4\text{-VP}]$ -PdNPs in Scheme 2. The formation of the polymer salt is approved with observation of the N–H stretching frequency at  $3415\text{ cm}^{-1}$  in the FT-IR of  $[\text{P}_4\text{-VP}]$ -PdNPs (b, in Fig. 3).

During our study, we found that, 1-h reflux is necessary for good dispersion of the polymer in the mixture to provide better interaction between the metal and the stabilizer to prevent agglomeration after reduction. When  $\text{H}_2\text{PdCl}_4$  in methanol is refluxed in the presence of  $[\text{P}_4\text{-VP}]$  2% DVB, probably the complexation takes place between  $\text{Pd}^{2+}$  ions and the nitrogen atoms of the pyridine pendant group of polymer [(I) in Scheme 2], and this can be to prevent the agglomeration after reduction of  $\text{Pd}^{2+}$  to  $\text{Pd}(0)$  occurs by  $\text{NaBH}_4$ .  $[\text{P}_4\text{-VP}]$ -PdNPs could be isolated as a dark brown solid from the reaction mixture by removing the volatiles in vacuum. Also as Fig. 3 reveals, the C=C ( $1414\text{ cm}^{-1}$ ) and C=N ( $1596\text{ cm}^{-1}$ ) stretching frequencies of pyridine pendant groups in  $[\text{P}_4\text{-VP}]$  2% DVB (a, in Fig. 3) and  $[\text{P}_4\text{-VP}]$ -PdNPs (b, in Fig. 3) are the same, and it can be concluded that the  $\text{Pd}^{2+}$  ions reduced to  $\text{Pd}(0)$  and absorbed on the surface or in the pores of the polymer, while upon polymer complexation with  $\text{Pd}^{2+}$  ions, the C=N and C=C stretching frequencies in vinylpyridine of catalyst must be shifted to higher frequencies as reported by Hasik et al. [71].

In order to obtain the microstructure of the  $[\text{P}_4\text{-VP}]$ -PdNPs nanocomposites, the typical TEM images (high resolution) are clearly shown in (Fig. 4a, b). It could be seen that the Pd nanoparticles in the range of 4–6 nm were uniformly attached on the surface of polymer.

The XRD diffraction patterns of  $[\text{P}_4\text{-VP}]$ -PdNPs are shown in Fig. 4c. Three observed peaks in XRD pattern at  $2\theta = 39, 46$  and  $69$  are attributed to elemental palladium. The diffraction peaks were broadened owing to the very small crystallite size. The random orientation of particles

**Fig. 3** FT-IR spectra of **a**  $[\text{P}_4\text{-VP}]$  2% DVB and **b**  $[\text{P}_4\text{-VP}]$ -PdNPs



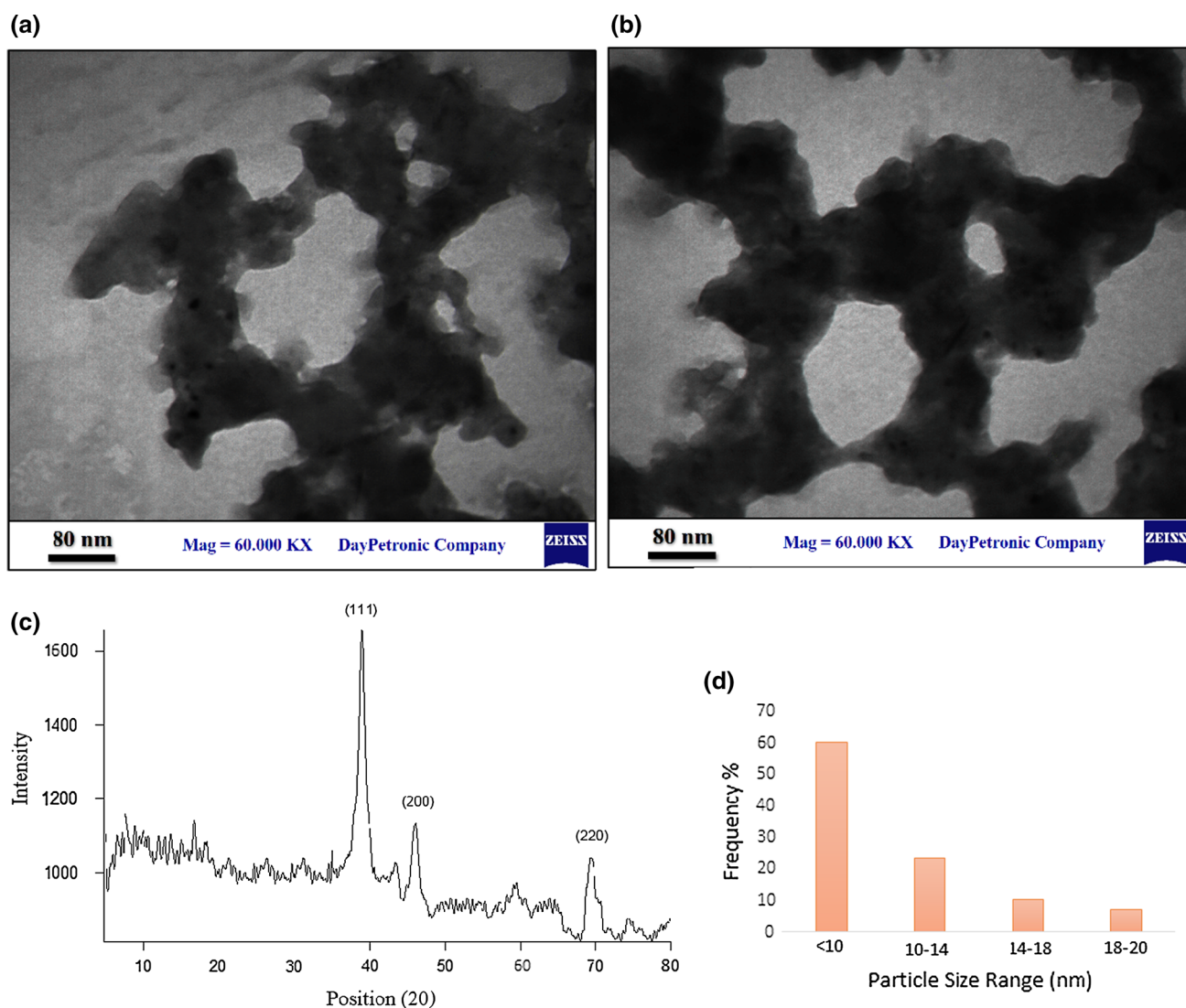


**Fig. 4** **a, b** TEM images, **c** XRD diffractogram of Pd nanoparticles in [P<sub>4</sub>-VP]-PdNPs and **d** nanoparticles size distributions

allows for a statistical measure of the size distribution to be generated (Fig. 4d).

The morphology of the [P<sub>4</sub>-VP]-PdNPs was studied by FESEM (at magnification of 100 KX) image (Fig. 5). One of the applications of FESEM includes small contamination feature geometry and elemental composition measurement. The FESEM micrographs of [P<sub>4</sub>-VP] 2% DVB after refluxed (1 h) in methanol in the presence of H<sub>2</sub>PdCl<sub>4</sub> before the addition of sodium borohydride do not show any Pd nanoparticles on the surface of the polymer [(a) in Fig. 5], while when [P<sub>4</sub>-VP] 2% DVB is refluxed (1 h) in ethanol in the presence of H<sub>2</sub>PdCl<sub>4</sub> before addition of sodium borohydride, the FESEM micrographs show the Pd nanoparticles on the surface of the polymer [(b) in Fig. 5]. This means that Pd<sup>2+</sup> reduces to Pd(0) by ethanol and stabilizes by polymer, and consequently, [P<sub>4</sub>-VP]-PdNPs

form. But, when sodium borohydride is added, reduction of Pd<sup>2+</sup> to Pd(0) by sodium borohydride and stabilization of Pd(0) by polymer occurs faster, and consequently, Pd nanoparticles in the [P<sub>4</sub>-VP]-PdNPs have very small size. In this case, the FESEM micrographs [(c) Fig. 5] show a large number of uniformly distributed Pd nanoparticles and have very small size distribution with a rough surface. After immersing these catalysts in organic solvents for a few days and then repeatedly washing with water and organic solvents (ethanol, toluene and acetone), the FESEM of these nanoparticles before and after the reaction are basically identical.

EDX analysis of [P<sub>4</sub>-VP]-PdNPs was used to analyze the composition of samples and is shown in Fig. 5e. This analysis shows considerable content of Pd (2.3%).



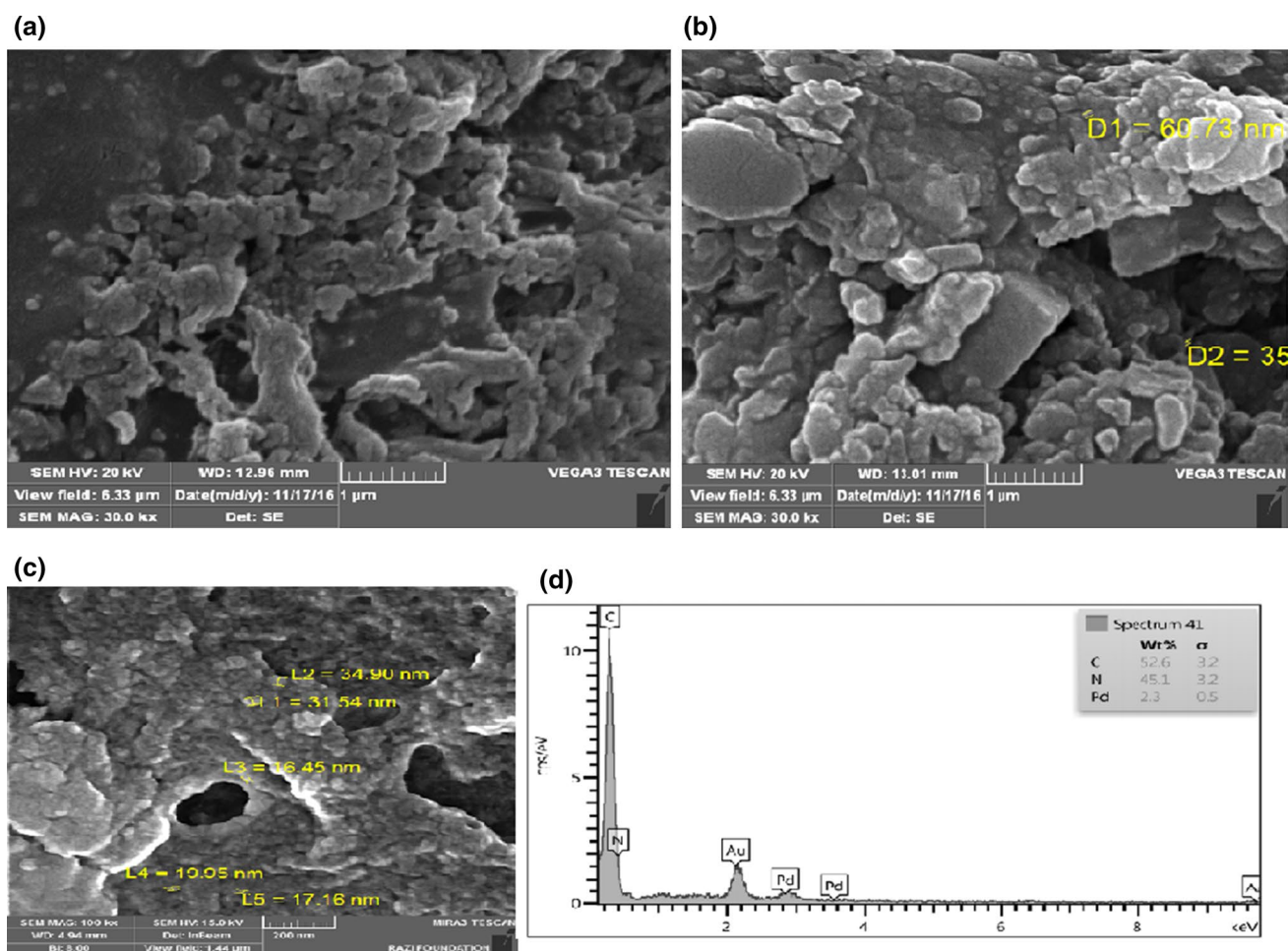
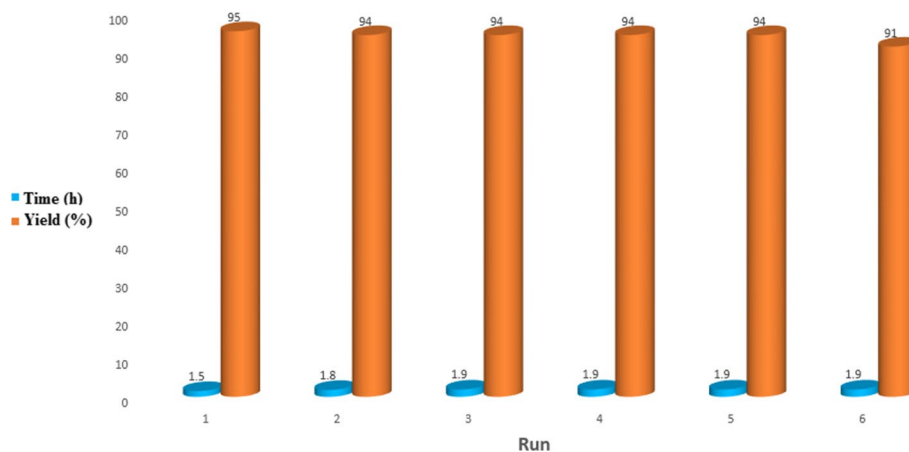


**Fig. 5** FESEM images of **a**  $[P_4\text{-VP}]$  2% DVB after refluxed (1 h) in methanol in the presence of  $\text{H}_2\text{PdCl}_4$  before the addition of sodium borohydride, **b**  $[P_4\text{-VP}]$  2% DVB after refluxed (1 h) in ethanol in the presence of  $\text{H}_2\text{PdCl}_4$  before the addition of sodium borohydride,

**c**  $[P_4\text{-VP}]$  2% DVB after refluxed (1 h) in methanol in the presence of  $\text{H}_2\text{PdCl}_4$  after the addition of sodium borohydride,  $[P_4\text{-VP}]$ -PdNPs and **d** EDX analysis of  $[P_4\text{-VP}]$ -PdNPs

**Fig. 6** Recovery studies: successively catalyzed by the same recovered  $[P_4\text{-VP}]$ -PdNPs under the same reaction conditions (model reaction)



However, the capacity of [P<sub>4</sub>-VP]-PdNPs was determined by AAS using Analytik Jena nova 300 (model 330, Germany). After the filtration of the mixture in step 2 for the synthesis of [P<sub>4</sub>-VP]-PdNPs, the excessive palladium ions in the filtrates determination were carried out on a Buck Scientific atomic absorption spectrometer (Model 210 VGP, USA) with a hollow cathode lamp using air-acetylene flame. The single-line flow-injection system consisting of peristaltic pump (Ismatic, MS-REGLO/8-100, Switzerland) and rotary injection valve (Rheodyne, CA, USA) with a loop of 100- $\mu$ L capacity was used for the effective control of the amount of sample and reproducibility of the measurements. The absorbance time response was monitored on an x-t-chart recorder (L-250), and consequently, the capacity of the polymer was determined to be 0.10 mmol of Pd g<sup>-1</sup> of the polymer.

After characterization of the catalyst structure, its catalytic activity was studied in coupling reaction between 1,2-diketones and 1,2-diamines for synthesis of pyrazines and quinoxalines and we found that [P<sub>4</sub>-VP]-PdNPs is as a suitable and reusable catalyst for synthesis of pyrazines and quinoxalines (Scheme 1).

In order to increase the yields of products, optimization of the reaction conditions was accomplished. Benzoin (1 mmol) and *o*-phenylenediamine (1.1 mmol), in the presence of [P<sub>4</sub>-VP]-PdNPs under heating in dimethyl formamide (DMF), were chosen as model reaction conditions and were converted to 2,3-diphenylquinoxaline product. The

model reaction behavior was studied under a variety of conditions, and the results are summarized in Table 1. First, we began to test in different solvents such as DMF (3 mL) in different temperatures and reflux in 3 mL of other solvents such as ethanol, methanol, acetonitrile, dichloromethane and chloroform, and the results are summarized in Table 1. During our optimization studies, it was found that 120 mg of [P<sub>4</sub>-VP]-PdNPs in 3 mL of DMF at 120 °C was the best conditions for complete conversion in a short reaction time, to achieve the highest yield of 2,3-diphenylquinoxaline product (Entry 3). The efficiency of the [P<sub>4</sub>-VP]-PdNPs compared to various catalysts was also examined (Table 1, entries 14–19), and it was found that [P<sub>4</sub>-VP]-PdNPs were an efficient and superior catalyst compared to other heterogeneous catalysts with respect to time and yield of product. During our optimization studies, we also found that the [P<sub>4</sub>-VP]-PdNPs (a dark brown color catalyst) are stable for months at room temperature. As Table 1 reveals, Pd(OAc)<sub>2</sub> and PdCl<sub>2</sub> reacted faster than [P<sub>4</sub>-VP]-PdNPs (entries 14 and 15) as expected, but they were not reusable catalysts.

After the optimized reaction conditions, the condensation reaction of 1,2-diamines such as ethylenediamine and different *o*-phenylenediamines with  $\alpha$ -hydroxyketones such as benzoin, furoin and aniso in was explored for the synthesis of a few pyrazine derivatives and various quinoxalines, and the results are summarized in Table 2. We have also successfully applied this new method on a nearly large scale;

**Table 1** Synthesis of 2,3-diphenylquinoxaline using benzoin and 1,2-phenylenediamine as a model reaction under various conditions

Entry	Catalyst (mol%)	Solvent	Temperature (°C)	Time (h)	Yield (%) <sup>a</sup>
1	[P <sub>4</sub> -VP]-PdNPs (0.012 mol%)	DMF	90	5	89
2	[P <sub>4</sub> -VP]-PdNPs (0.012 mol%)	DMF	100	2.5	92
3	[P <sub>4</sub> -VP]-PdNPs (0.012 mol%)	DMF	110	1.5	95
4	[P <sub>4</sub> -VP]-PdNPs (0.012 mol%)	DMF	120	1.5	90
5	[P <sub>4</sub> -VP]-PdNPs (0.012 mol%)	DMF	130	1.6	85
6	[P <sub>4</sub> -VP]-PdNPs (0.013 mol%)	DMF	110	1.5	95
7	[P <sub>4</sub> -VP]-PdNPs (0.011 mol%)	DMF	110	1.8	90
8	[P <sub>4</sub> -VP]-PdNPs (0.010 mol%)	DMF	110	2	91
9	[P <sub>4</sub> -VP]-PdNPs (0.012 mol%)	EtOH	Reflux	5	91
10	[P <sub>4</sub> -VP]-PdNPs (0.012 mol%)	MeOH	Reflux	7	80
11	[P <sub>4</sub> -VP]-PdNPs (0.012 mol%)	CH <sub>3</sub> CN	Reflux	10	82
12	[P <sub>4</sub> -VP]-PdNPs (0.012 mol%)	CHCl <sub>3</sub>	Reflux	10	85
13	[P <sub>4</sub> -VP]-PdNPs (0.012 mol%)	CH <sub>2</sub> Cl <sub>2</sub>	Reflux	12	60
14	Pd(OAc) <sub>2</sub> (3)	DMF	110	0.5	97
15	PdCl <sub>2</sub> (2.3)	DMF	110	0.5	97
16	H <sub>2</sub> PdCl <sub>4</sub> (3.4)	DMF	110	2.5	70
17	[P <sub>4</sub> -VP] 2% DVB (0.012 mol%)	DMF	110	7	80
18	[P <sub>4</sub> -VP]-ZnCl <sub>2</sub> (0.012 mol%)	DMF	110	4	92
19	[P <sub>4</sub> -VP]-CuI (0.012 mol%)	DMF	110	4	90

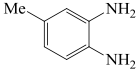
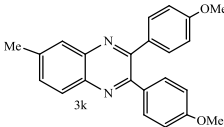
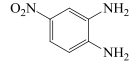
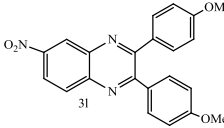
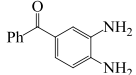
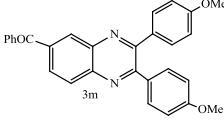
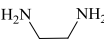
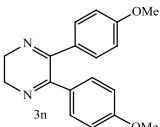
All the reactions were performed using benzoin (1 mmol) and 1,2-phenylenediamine (1.1 mmol) under heating in a solvent

<sup>a</sup>Yields refer to isolated pure product

**Table 2** Synthesis of pyrazine and quinoxaline derivatives from  $\alpha$ -hydroxyketones (1 mmol) and 1,2-diamines (1.1 mmol) using  $[P_4-VP]-PdNPs$  (0.0120 mol%) in DMF at 110 °C

Entry	$\alpha$ -Hydroxyketone	Diamine	Product	Time (min)	Yield <sup>a</sup> (%)
1	Benzoin			1.5	95
2	Benzoin			1.3	97
3	Benzoin			7	95
4	Benzoin			6	95
5	Benzoin			0.5	96
6	Furoin			1.2	89
7	Furoin			0.8	99
8	Furoin			5	97
9	Furoin			4.5	95
10	Anisoin			7	94

Table 2 (continued)

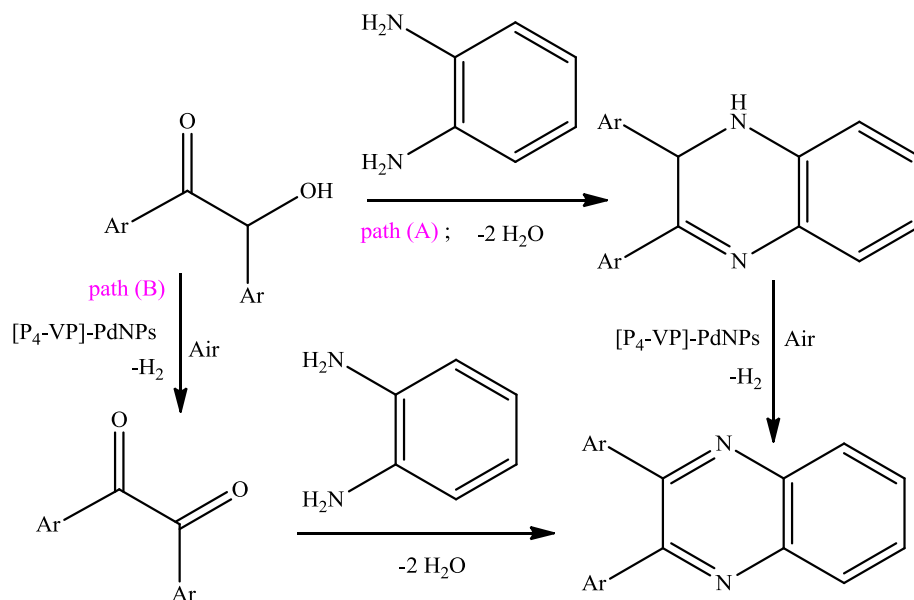
11	Anisoin			5	94
12	Anisoin			11	87
13	Anisoin			12	81
14	Anisoin			0.5	98

<sup>a</sup>Isolated yields

for example, up to 15 mmoles of benzoin and *o*-phenylenediamine (Table 2, entry 1) could be converted into the corresponding quinoxaline product (**3a**) in 95% isolated yield. In general, all reactions were very clean and the products were obtained in high–excellent yields (81–99%). All the products were cleanly isolated with simple filtration and precipitation in water. All products were characterized by FT-IR, <sup>1</sup>H and <sup>13</sup>C NMR spectra, melting point and compared with literature data.

As Table 2 reveals, both electron-rich and electron-deficient *o*-phenylenediamines were effective in this process. When *o*-phenylenediamines are substituted at the 4-position with electron-donating groups, higher rates and yields are observed than the ones bearing electron-withdrawing groups at that position (entries 2–4, 7–9 and 11–13). For example, 4-nitro-1,2-phenylenediamine afforded the product in 6 h with 95% yield, when reacted with benzoin (entry 4), with furoin in 4.5 h with 95% yield (entry 9) and with

Scheme 3 The plausible mechanism of the reaction



anisoin in 11 h with 87% yield (entry 12), while 4-methyl-1,2-phenylenediamine afforded the product in 1.3 h with 97% yield (entry 2), with furoin in 0.8 h with 99% yield (entry 7) and with anisoin in 5 h with 94% yield (entry 11). All the reactions proceeded very efficiently and no undesirable side-reactions were observed, although the yields were highly dependent on the substrate used.

The main advantage of polymer-supported catalyst is its insolubility in the reaction medium and consequently its easier work-up by a simple filtration. A few pyrazine derivatives such as 2,3-dihydro-5,6-diphenylpyrazine and 5,6-bis-(4-methoxyphenyl)-2,3-dihydro-pyrazin and various quinoxalines were prepared by coupling reaction of 1,2-diamines and  $\alpha$ -hydroxyketones. The process is experimentally simple and appears to have enormous scope.

The reusability of the catalyst was investigated.  $[P_4\text{-VP}]\text{-PdNPs}$  can be easily recovered and reused many times without significant loss of catalytic activity. After

completion of the model reaction, the recovered catalyst was washed with DMF and after dryness was reused in the next similar run. This procedure was repeated for 6 consecutive runs, and the results of this study are shown in Fig. 5. As Fig. 5 reveals, when the polymer was reused after six runs in the same reaction and under identical conditions, the isolated yield of the product was decreased only a few percent (4.2%) which indicates the low leaching amount of Pd catalyst into the reaction mixture. No decomposition of the stabilizer was observed in the reaction, and  $[P_4\text{-VP}]\text{-PdNPs}$  are found to be stable to metal leaching throughout the reaction. Moreover, the recyclability of the supported catalyst is also important.

Based on the previous reports, our observations and obtained results, the plausible mechanism of the reaction catalyzed by  $[P_4\text{-VP}]\text{-PdNPs}$  is shown in Scheme 3. In path (A),  $[P_4\text{-VP}]\text{-PdNPs}$  promoted the condensation reaction of 1,2-diamine and  $\alpha$ -hydroxyketone via cyclization and dehydration, and consequently, the corresponding

**Table 3** Comparison of the model reaction with other reported methods for synthesis of 2,3-diphenylquinoxaline

Entry	Reaction conditions	Time (h)	Yield (%) <sup>a</sup>	References
1	$[(\text{NH}_4)_6\text{Mo}_7\text{O}_{24}\cdot 4\text{H}_2\text{O}\text{-PEG 300}]$ , MWI <sup>b</sup> (420 W)/90 °C	0.25	98	[14]
2	AcOH, reflux	2	96	[19]
3	$\text{Ga}(\text{ClO}_4)_3$ , EtOH, reflux	4	70	[77]
4	Yb/NaY, HOAc, 80 °C	4	85	[78]
5	Yb/NaY, morpholine (35 mol%), HOAc, 80 °C	4	93	[78]
6	Yb/NaY, $\text{PhI}(\text{OAc})_2$ (35 mol%), 80 °C	4	83	[78]
7	Au-NPs, $\text{K}_2\text{CO}_3$ , $\text{H}_2\text{O}$ , air, 80 °C	4	91	[79]
8	Au-CNT <sup>c</sup> , toluene/ $\text{H}_2\text{O}$ (1/1)/NaOH, r.t.	26	96	[80]
9	CaO (5 mol%), ethylene glycol, $\text{O}_2$ (1 atm.), 130 °C	6	93	[81]
10	K-OMS-2 catalysts, toluene, reflux	1	47	[82]
11	$\text{CH}_3\text{CN}$ , $\text{O}_2$ , reflux	3	20	[83]
	$\text{CH}_3\text{CN}$ , $\text{O}_2$ , $\text{FeCl}_3$ , reflux	3	30	[83]
12	$\text{CH}_3\text{CN}$ , $\text{O}_2$ , MPA <sup>d</sup> , reflux	3	50	[83]
13	$\text{CH}_3\text{CN}$ , $\text{O}_2$ , FeMPA, reflux	3	95	[83]
14	$\text{CH}_3\text{CN}$ , $\text{O}_2$ , $\text{Fe}(\text{NO}_3)_3$ , reflux	3	25	[83]
15	L-proline, air, $\text{H}_2\text{O}$ , reflux	12	87	[84]
16	$\text{FeCl}_3$ (10 mol%), morpholine (20 mol%), EtOH, 80 °C	1.5	95	[85]
17	Fe-molybdophosphoric acid (50 mg)/ $\text{O}_2$ / $\text{CH}_2\text{Cl}_2$ /reflux	3	95	[83]
18	Amberlite IR-120H (200 mg), 110 °C	5	95	[86]
19	MW (15 min), open vessel	0.25	34	[87]
20	MW (15 min), closed vessel	0.25	74	[87]
21	$\text{I}_2$ (25 mol%), DMSO (2 mL), 100 °C	22	92	[88]
22	$\text{Pd}(\text{OAc})_2$ (2 mol%)/MS <sup>f</sup> /toluene/ $\text{Et}_3\text{N}$ /THF/reflux	24	72	[89]
23	$[P_4\text{-VP}]\text{-PdNPs}$ (1.2 mol%), DMF/120 °C	1.5	95	g

<sup>a</sup>Yields refer to isolated products

<sup>b</sup>MWI microwave irradiation

<sup>c</sup>CNT carbon nanotube

<sup>d</sup>MPA 12-molybdophosphoric acid

<sup>e</sup>PTSA para-toluenesulfonic acid

<sup>f</sup>MS molecular sieves

<sup>g</sup>Present method (Table 2, entry 1)

1,2-dihydroquinoxaline is produced. Then, aerobic oxidation of 1,2-dihydroquinoxaline in the presence of [P<sub>4</sub>-VP]-PdNPs occurs and the corresponding quinoxaline product is produced. In path (B), benzoin is oxidized to benzil by aerobic oxidation in the presence of [P<sub>4</sub>-VP]-PdNPs and then by condensation reaction of 1,2-diamine and benzil, via cyclization and dehydration, and consequently the corresponding quinoxaline formation occurs (Scheme 3). In fact, the reaction occurs on the surface or in the pores of the polymer.

In order to show the advantages and limitations of this protocol, we have compared the results of our model reaction with those reported in the literature (Table 3). [P<sub>4</sub>-VP]-PdNPs are an effective catalyst for this reaction in terms of the amount of catalyst (1.2 mol%) and the reaction time (1.5 h) in comparison with other catalysts [14, 19, 77–88].

The superiority of this work is that catalyst is recoverable and reusable for many times without significant loss of their activity. However, the yield of the product and the reaction time of our procedure are comparable with reported methods, while the reaction time for our method is shorter than many of the other previously reported methods. This can probably be attributed to the local concentration of palladium nanoparticle species on the surface or inside the pores of the polymer that can be interacted with 1,2-diamines and  $\alpha$ -hydroxyketones or benzoin (Scheme 3).

## Conclusions

In conclusion, we have developed a simple and green procedure for the synthesis of pyrazines and quinoxalines via condensation reaction between 1,2-diamines and  $\alpha$ -hydroxyketones in the presence of recyclable new polymeric catalyst, [P<sub>4</sub>-VP]-PdNPs.

The main advantage of polymeric catalysts over no polymeric catalysts is their insolubility in the reaction medium and consequently their easier work-up by a simple filtration. The introduced catalyst can promote the yields and reaction times for many repeated runs with very low leaching amounts of supported catalyst into the reaction mixture. Moreover, high yields of products, short reaction times and ease of work-up will make the present method a useful and important addition to the previous methodologies for the synthesis of quinoxalines. In addition, there is current research and general interest in heterogeneous systems because such systems have importance in industry and in developing technologies [90]. On the other hand, polymeric reagents would be particularly attractive since they can be recovered by filtration and can be used again.

## References

1. D. Sherman, J. Kawakami, H.Y. He, F. Dhun, R. Rios, H. Liu, W. Pan, Y.J. Xu, S.P. Hong, M. Arbour, M. Labelle, M.A.J. Dunton, *Tetrahedron Lett.* **48**, 8943 (2007)
2. J.A. Pereira, A.M. Pessoa, M.N.D.S. Cordeiro, R. Fernandes, C. Prudencio, J.P. Noronha, M. Vierira, *Euro. J. Med. Chem.* **97**, 664 (2015)
3. L.M. Wilhelmsson, N. Kingi, J. Bergman, *J. Med. Chem.* **51**, 7744 (2008)
4. Q. Weng, D. Wang, P. Guo, L. Fang, Y. Hu, Q. He, B. Yang, *Euro. J. Pharmacol.* **581**, 262 (2008)
5. Y. Xu, F. Wu, Z. Yao, M. Zhang, S. Jiang, *Molecules* **16**, 6894 (2011)
6. C.H. Sridevi, K. Balaji, A. Naidu, R. Sudhakaran, *Euro. J. Chem.* **7**, 234 (2010)
7. A. Dell, D.H. William, H.R. Morris, G.A. Smith, J. Feeney, G.C.K. Roberts, *J. Am. Chem. Soc.* **97**, 2497 (1975)
8. S.A. Raw, C.D. Wilfred, R.J.K. Taylor, *Chem. Commun.* **18**, 2286 (2003)
9. A. Kumar, S. Kumar, A. Saxena, A. De, S. Mozumdar, *Catal. Commun.* **9**(5), 778 (2008)
10. J.Y. Jaung, *Dyes Pigments* **71**, 45 (2006)
11. S. Dailey, W.J. Feast, R.J. Peace, I.C. Sage, S. Till, E.L. Wood, *J. Mater. Chem.* **11**, 2238 (2001)
12. T.R.J. Thomas, K.M. Velusamy, J.T. Lin, C.H. Chuen, Y.T. Tao, *Chem. Mater.* **17**, 1860 (2005)
13. M.J. Crossley, L.A. Johnston, *Chem. Commun.* **10**, 1122 (2002)
14. K. Aghapoor, F. Mohsenzadeh, M. Mohebi Morad, H.R. Darabi, *Transit. C. R. Chimie* **15**, 764 (2012)
15. C. Srinivas, C.N.S.S.P. Kumar, V.J. Rao, S. Palaniappan, *J. Mol. Catal. A Chem.* **265**, 227 (2007)
16. B.A.D.S. Neto, A.S. Lopes, M. Wust, V.E.U. Costa, G. Ebeling, J. Dupont, *J. Tetrahedron Lett.* **46**, 6843 (2005)
17. H.R. Darabi, F. Tahoori, K. Aghapoor, F. Taala, F. Mohsenzadeh, *J. Braz. Chem. Soc.* **19**, 1646 (2008)
18. J.J. Cai, J.P. Zou, X.Q. Pan, W. Zhang, *Tetrahedron Lett.* **49**, 7386 (2008)
19. M.R. Islami, Z. Hassani, *Arkivoc* **xv**, 280 (2008)
20. D.J. Brown, *Quinoxalines: Supplement II, The Chemistry of Heterocyclic Compounds* (Wiley, New Jersey, 2004)
21. S.Y. Kim, K.H. Park, Y.K. Chung, *Chem. Commun.* **10**, 1321 (2005)
22. S. Antoniotti, E. Donach, *Tetrahedron Lett.* **43**, 3971 (2002)
23. D. Aparicio, O.A. Attanasi, P. Filippone, R. Ignacio, S. Lillini, F. Mantellini, F. Palacios, J.M. Santos, *J. Org. Chem.* **71**, 5897 (2006)
24. Z. Wu, N.J. Ede, *Tetrahedron Lett.* **42**, 8115 (2001)
25. S.K. Singh, P. Gupta, S. Duggineni, B. Kundu, *Synlett* **2003**, 2147 (2003)
26. R.S. Robinson, R.J.K. Taylor, *Synlett* **2005**, 1003 (2005)
27. M. Beller, H. Fischer, K. Kuhlein, C.P. Reisinger, W.A. Hermann, *J. Organomet. Chem.* **520**, 257 (1996)
28. C.P. Mehnert, J.Y. Ying, *Chem. Commun.* 2215 (1997)
29. D.C. Sherrington, P. Hodge, *Synthesis and Separations Using Functional Polymers* (Wiley, New York, 1988)
30. A. Akelah, D.C. Sherrington, *Polymer* **24**, 1369 (1984)
31. S.V. Ley, I.R. Baxendale, R.N. Bream, P.S. Jackson, A.G. Leach, D.A. Longbottom, M. Nesi, J.S. Scott, R.I. Storer, S.J. Taylor, *J. Chem. Soc. Perkin Trans.* **1**, 3815 (2000)
32. M.A. Karimi Zarchi, R. Nabaei, S. Barani, *J. Appl. Polym. Sci.* **123**, 788 (2012)
33. M.A. Karimi Zarchi, R. Nabaei, *J. Appl. Polym. Sci.* **124**, 2362 (2012)

34. M.A. Karimi Zarchi, S. Barani, *Chinese. J. Polym. Sci.* **31**, 1002 (2013)
35. M.A. Karimi Zarchi, F. Nazem, *J. Appl. Polym. Sci.* **123**, 1977 (2012)
36. M.A. Karimi Zarchi, F. Nazem, *J. Iran. Chem. Soc.* **11**, 91 (2014)
37. M.A. Karimi Zarchi, F. Nazem, *J. Iran. Chem. Soc.* **11**, 1731 (2014)
38. M.A. Karimi Zarchi, Z. Escandari, *J. Appl. Polym. Sci.* **121**, 1916 (2011)
39. M.A. Karimi Zarchi, N. Ebrahimi, *J. Appl. Polym. Sci.* **121**, 2621 (2011)
40. M.A. Karimi Zarchi, N. Ebrahimi, *J. Appl. Polym. Sci.* **124**, 2807 (2012)
41. M.A. Karimi Zarchi, N. Ebrahimi, *Iran. Polym. J.* **21**, 591 (2012)
42. M.A. Karimi Zarchi, N. Ebrahimi, *J. Appl. Polym. Sci.* **125**, 2163 (2012)
43. M.A. Karimi Zarchi, N. Ebrahimi, *Phosphorous Sulfur Silicon Relat. Elem.* **187**, 1226 (2012)
44. M.A. Karimi Zarchi, R. Banihashemi, *Phosphorous Sulfur Silicon Relat. Elem.* **189**, 1378 (2014)
45. M.A. Karimi Zarchi, A. Tarabsaz, *Phosphorous Sulfur Silicon Relat. Elem.* **190**, 550 (2015)
46. M.A. Karimi Zarchi, A. Tarabsaz, *J. Polym. Res.* **20**, 208 (2013)
47. M.A. Karimi Zarchi, A. Tarabsaz, *Chin. J. Polym. Sci.* **31**, 1660 (2013)
48. M.A. Karimi Zarchi, A. Tabatabaei Bafghi, *J. Sulfur Chem.* **36**, 403 (2015)
49. M.A. Karimi Zarchi, S.Z. Mousavi, *J. Polym. Sci.* **21**, 330 (2014)
50. M.A. Karimi Zarchi, R. Banihashemi, *J. Sulfur Chem.* **37**, 282 (2016)
51. L.D. Rampino, F.F. Nord, *J. Am. Chem. Soc.* **63**, 2745 (1941)
52. Y. Li, X.M. Hong, D.M. Collard, M.A. El-Sayed, *Org. Lett.* **2**, 2385 (2000)
53. D.D.L. Martins, H.M. Alvarez, L.C.S. Aguiar, *Tetrahedron Lett.* **51**, 6814 (2010)
54. Y. Li, E. Boone, M.A. El-Sayed, *Langmuir* **18**, 4921 (2002)
55. K.A. Guy, J.R. Shapley, *Organometallics* **28**, 4020 (2009)
56. R. Narayanan, M.A. El-Sayed, *J. Am. Chem. Soc.* **125**, 8340 (2003)
57. J.L. Lan, C.C. Wan, Y.Y. Wang, *J. Electrochem. Soc.* **155**, K77 (2008)
58. P. Li, L. Wang, H. Li, *Tetrahedron* **61**, 8633 (2005)
59. A. Gniewek, A.M. Trzeciak, J.J. Ziolkowski, L. Kepinski, J. Wrzyszczyk, W. Tylus, *J. Catal.* **229**, 332 (2005)
60. D.D.L. Martins, H.M. Alvarez, L.C.S. Aguiar, O.A.C. Antunes, *Appl. Catal. A Gener.* **408**, 47 (2011)
61. A. Drelinkiewicz, M. Hasik, *J. Mol. Catal. A Chem.* **177**, 149 (2001)
62. A.L.F.D. Souza, L.C.D. Silva, B.L. Oliveira, O.A.C. Antunes, *Tetrahedron Lett.* **49**, 3895 (2008)
63. K.A. Guy, H. Xu, J.C. Yang, C.J. Werth, J.R. Shapley, *J. Phys. Chem. C* **113**, 8177 (2009)
64. F. Durap, O. Metin, M. Aydemir, S. Ozkar, *Appl. Organomet. Chem.* **23**, 498 (2009)
65. C. Evangelisti, N. Panziera, A.D. Alessio, L. Bertinetti, M. Botavina, *J. Catal.* **272**, 246 (2010)
66. B. Tamami, H. Allahyari, S. Ghasemi, F. Farjadian, *J. Organomet. Chem.* **696**, 594 (2011)
67. J. Zou, K.S. Iyer, S.G. Stewart, C.L. Raston, *New J. Chem.* **35**, 854 (2011)
68. D. Shah, H. Kaur, *Curr. Catal.* **3**, 39 (2014)
69. Y. Zhao, J.A. Baeza, N.K. Rao, L. Calvo, M.A. Gilarranz, Y.D. Li, L. Lefferts, *J. Catal.* **318**, 162 (2014)
70. M. Abdollahi-Alibeik, E. Heidari-Torkabad, *C. R. Chim.* **15**, 517 (2012)
71. K. Niknam, D. Saberi, M. Mohagheghnejad, *Molecules* **14**, 1915 (2009)
72. H.A. Oskooie, M.M. Heravi, K. Bakhtiari, M.H. Tehrani, *Monatsh. Chem.* **138**, 875 (2007)
73. W.X. Guo, H.L. Jin, J.X. Chen, F. Chen, J.C. Ding, H.Y. Wu, *J. Braz. Chem. Soc.* **20**, 1674 (2009)
74. M.M. Heravi, M.H. Tehrani, K. Bakhtiari, H.A. Oskooie, *Catal. Commun.* **8**, 1341 (2007)
75. A.L. Santana, L.K. Noda, A.N.T. Pires, J.R. Bertoline, *Polym. Test* **23**, 839 (2004)
76. A. Drelinkiewicz, M. Hasik, S. Quillard, C. Paluszkiwicz, *J. Mol. Struct.* **511–512**, 205 (1999)
77. F. Pan, T.M. Chen, J.J. Cao, J.P. Zou, W. Zhang, *Tetrahedron Lett.* **53**, 2508 (2012)
78. L.Y. Fan, L. Wei, W.J. Hua, X.X. Li, *Chin. Chem. Lett.* **25**, 1203 (2014)
79. T. Bhattacharya, T.K. Sarma, S. Samanta, *Catal. Sci. Technol.* **2**, 2216 (2012)
80. N. Shah, E. Gravel, D.V. Jawale, E. Doris, I.N.N. Namboothiri, *Chem. Cat. Chem.* **6**, 719 (2014)
81. T. Hara, Y. Takami, N. Ichikuni, S. Shimazu, *Chem. Lett.* **41**, 488 (2012)
82. S. Sithambaram, Y. Ding, W. Li, X. Shen, F. Gaenzler, S.L. Suib, *Green Chem.* **10**, 1029 (2008)
83. K.T.V. Rao, P.S.S. Prasad, N. Lingaiah, *J. Mol. Catal. A Chem.* **312**, 65 (2009)
84. A. Kamal, K.S. Babu, S. Faazil, S.M. Ali Hussaini, A.B. Shaik, *RSC Adv.* **4**, 46369 (2014)
85. W. Song, P. Liu, M. Lei, H. You, X. Chen, H. Chen, L. Ma, L. Hu, *Synth. Commun.* **42**, 236 (2012)
86. A. Kamal, K.S. Babu, S.M. Ali Hussaini, R. Mahesh, A. Alarifi, *Tetrahedron Lett.* **56**, 2803 (2015)
87. V. Jeena, R.S. Robinson, *Tetrahedron Lett.* **55**, 642 (2014)
88. C. Xie, Z. Zhang, B. Yang, G. Song, H. Gao, L. Wen, C. Ma, *Tetrahedron* **71**, 1831 (2015)
89. R.S. Robinson, R.J.K. Taylor, *Synlett* **6**, 1003 (2005)
90. N.J. Turro, *Tetrahedron* **43**, 1589 (1987)